

RESONANCES AND TIME-OF-FLIGHT: ULTRASONIC PROBES OF CONDENSED MATTER GO DIGITAL

Albert Migliori

National High Magnetic Field Laboratory, Los Alamos National Laboratory
Los Alamos, New Mexico 87545

Introduction

Perhaps the speed of sound is one of the most fundamental and most often measured attributes of a solid. Acoustic students have been doing such measurements for years, seldom appreciating the wealth of knowledge that can be obtained from the solid from this apparently simple experiment. But to understand exactly what has been measured, what has influenced the measurement, how best to perform the measurement, and how accurately the measurement has been taken has often demanded a lifetime of experience. This paper describes some of the latest techniques that condensed matter physicists now use to probe solids.

The elastic stiffnesses of a solid can be determined with outstanding precision. Together with density, the stiffnesses control the speed of propagation of stress waves (sound) and depend on the variation of fundamental thermodynamic quantities—internal energy or free energy—with deformation. Unlike most of the quantities used to characterize condensed matter, the elastic moduli are fourth-rank tensors containing a wealth of detail, directional information, and consistency constraints that provide one of the most revealing probes of solids. Let us review this briefly by expanding on the concepts underlying stiffness, thermodynamics, and deformation in solids, and then examine two advances in measurement techniques.

The microscopic complexity of crystalline solids, as opposed to a gas or a liquid, reveals that many independent elastic moduli are present. This complicates everything. For example, in a triclinic crystal, the shape and structure of a unit cell includes nothing at right angles to anything else. A consequence of the tensor description of elasticity is that there are 21 independent elastic moduli, and there are no elastic waves for which displacements of atoms are either parallel to (compression) or perpendicular to (shear) the propagation direction.¹ The situation is worse if the time-reversal symmetry-breaking of a magnetic field is present. This all occurs because any stress applied to a solid's surface can be decomposed into two shear components parallel to the surface and a compressional one perpendicular in each of the three spatial directions for a total of 9 stress components. With the corresponding nine strain components, the Hooke's law matrix connecting stress to strain must have 81 components. However, time reversal symmetry and shear symmetry under interchange of coordinates requires a constrained symmetric matrix. Thus the total in zero magnetic field is

“Recently, full utilization of digitally generated and acquired signals has made possible advances in measurement techniques for both Pulse Echo (PE) and Resonant Ultrasound Spectroscopy (RUS) that are not possible with purely analog systems.”

reduced to 21 (the maximum number of independent entries in a symmetric 6x6 matrix). Even in a simple cubic crystal, three moduli are required, and only in special directions can elastic waves be called shear or compressional. Therefore, a complete measurement of the elastic stiffness tensor of a solid requires a lot of work

In well-behaved solids, the effects of very small strains are reversible and the state of the solid in thermal equilibrium uniquely relates pressure, volume, and temperature via the equation of state (EOS). Changing both volume and pressure, for example, forces a unique change in temperature. For shear waves, the EOS does not come into play because there are no volume changes during propagation. But for compressional waves, the volume change between the compressed and expanded parts of a single cycle of sound can produce small temperature differences. Rather oddly, these temperature differences disappear at very high frequency. The root of this is that the thermal penetration depth δ_K , the characteristic length for decay of temperature changes, varies inversely as the square root of the frequency, while the wavelength λ is proportional to the inverse of frequency. Thus λ becomes shorter than δ_K at high frequency, permitting nearly instantaneous thermal equilibration. This has important consequences—there are two longitudinal sound speeds, isothermal and adiabatic, and the adiabatic sound speed, the one usually measured by both time-of-flight and resonance techniques, depends on the thermodynamic internal energy, not the free energy as in isothermal sound.

The adiabatic elastic moduli are often the very first prediction of any theory of the electronic structure of a solid because the theorist needs only to change the distance between atoms (the volume) and rerun the code to get the moduli. Thus adiabatic sound speeds provide an important test of electronic structure while all elastic wave speeds provide crucial characterization of phase changes (when the solid changes from one set of attributes to another).

For these and many other reasons, the measurement of the elastic moduli of solids has a long and glorious tradition with many methods used, ranging from neutron scattering to optical spectroscopies. But the two most widely used methods are the time of flight (TOF) of an acoustic pulse² (pulse-echo (PE)) and frequency of resonances (resonant ultrasound spectroscopy (RUS)), both extensively reviewed elsewhere.³⁻⁸ Both methods use readily available hardware and



Fig. 1. An RUS probe used to 290mK and 15T. The small metallic sample is just resting on the lower transducer, while the upper transducer is also only making contact with its own weight.

are accessible to everyone. Also both methods have deep similarities based on the most precisely measured quantities in all of science. Those quantities—frequency and time—are used by both PE and RUS. For PE, the time of flight of an acoustic pulse is measured by counting the number of cycles of a stable oscillator that pass during transit of the pulse through the specimen. For RUS, the frequency at maximum response of a specimen resonance is measured by subdividing the frequency of a precision oscillator, effectively a timing measurement. In Fig. 1 we show an RUS probe for use at low temperatures, and in Fig. 2 we show typical echoes from a PE system.

Let us compare the applicability of the two methods. For both methods, the specimen must have very accurate geometry and crystallographic orientation. For PE, transducers must be carefully bonded. This permits measurements at high pressure because the specimen and transducer can be a pressure vessel. For RUS, only weak contact is needed but is also required, making it easy to make a simple measurement but essentially impossible to use at other than pressures. RUS obtains the entire elastic tensor in one measurement, while PE requires a separate measurement and transducer location for each modulus. PE almost always gives a correct result that can be analyzed using a pocket calculator while RUS can give spurious results and requires a complex computer code⁹ for analysis.

Recently, full utilization of digitally generated and acquired signals has made possible advances in measurement techniques for both PE and RUS that are not possible with purely analog systems. We describe here two key processes, one for PE, and one for RUS, that address the speed and noise issues in acquiring resonance data for RUS, and the ambiguity in determining the exact timing of an echoed pulse for PE.

Fast acquisition of swept-frequency RUS scans using digital signal processing

It is amusing to realize that all our laboratory work can be described as an analog to digital conversion because we begin with the analog processes to be studied and end with a file on a computer. Before we write a paper though, there is often an electronic conversion of some analog signal to a digital approximation of it (A/D). This process is necessarily constrained in many ways, not the least of which is that we must use commercially available A/D converters that are limited in speed, number of bits of precision, and have noise above the thermodynamic Johnson limit because of the com-

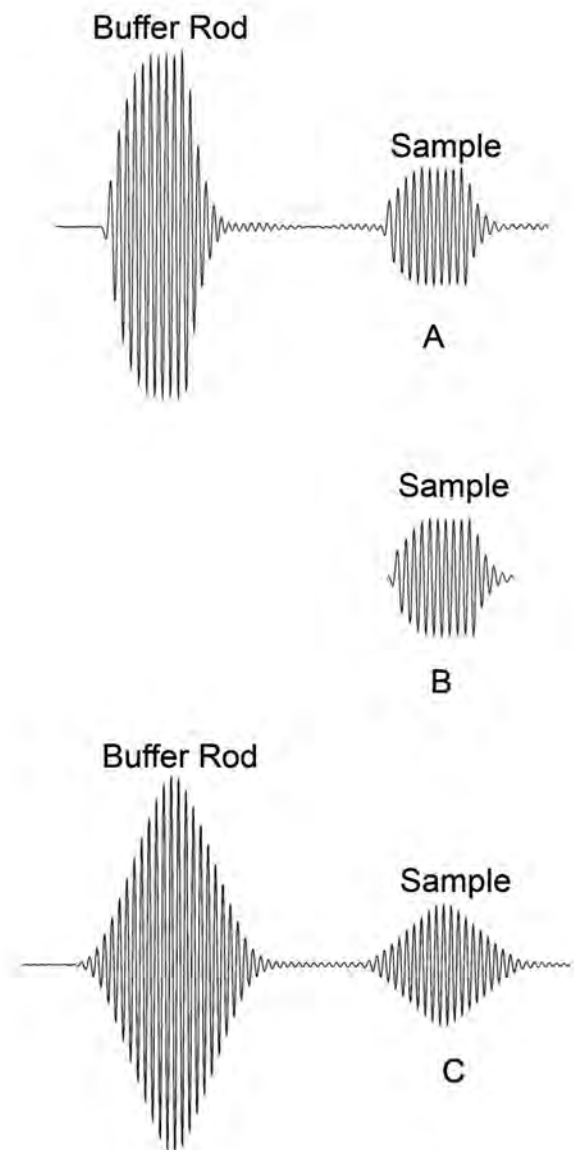


Fig. 2. Shown are: a) raw echoes from sample (S) and buffer rod (BR); b) the sample echo; and c) the convoluted echoes as described in the text.

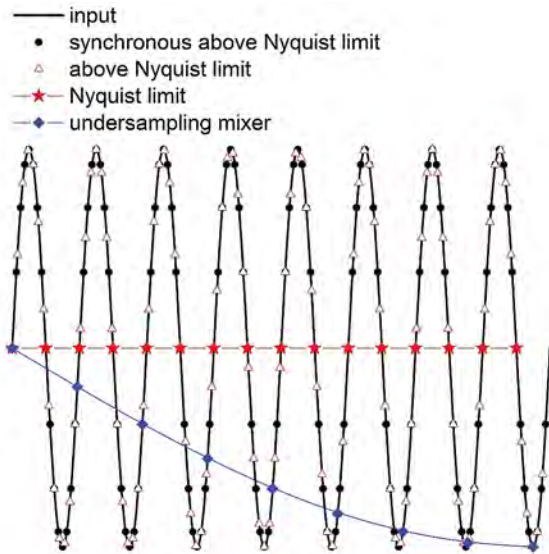


Fig. 3. Shown are the sampling points of an A/D converter under several scenarios, described in the text.

plexity of design while attempting to control cost. For these and other reasons, we (usually) want to input a signal to the A/D converter whose intrinsic noise is greater than the resolution of the A/D, and whose bandwidth is less than the Nyquist limit, the lowest “sampling frequency” that can be used. In Fig. 3, a noise-free sinusoidal signal of frequency f is digitized under several scenarios to illustrate the Nyquist-limit problem. Rather than offer a proof, let us find special cases that describe successes and failures in a digital capture of the signal. First we consider the Nyquist limit $f_N = 2f$. At this A/D sampling rate it is possible to miss completely the presence of the signal, as shown by the red stars in Fig. 3. Thus $2f$ is the absolute lower sampling rate bound for digital acquisition of an analog signal. As sampling rate increases above f_N (red triangles) we obtain an increasingly accurate digital representation of the signal. That is, just above f_N , every zero crossing of the signal is captured, even if, when we connect the dots, the signal is distorted until we heavily “oversample.” Thus a Fourier transform must contain the fundamental frequency in it. Below f_N (blue dots) “aliasing” occurs and we obtain a spurious representation that is the difference between an integer multiple of sampling rate and f (this process implements an under-sampling mixer used, among other places, in cell phone radio receivers). More simply, we missed some zero crossings, therefore the Fourier transform of the signal cannot have the actual fundamental frequency in it, only frequencies below f .

The sampling rate that will be discussed and that will be used for RUS is a special one indicated by the black dots in Fig. 3. The goal is to obtain the amplitude and phase of the sinusoidal signal with maximum speed and a useful noise floor, while rejecting other frequencies. The black dots are at a synchronous digitization (SD) rate that samples the signal at an integer multiple m of the fundamental frequency. The advantage of doing this is that for each cycle of the fundamental, it does not matter where one starts digitizing with respect to the phase of the signal, the set of numbers obtained after an integer multiple of m acquisitions is the same. Try it yourself with Fig. 3. Leave off the first black dot at the start,

but then you must add one more black dot at the end to preserve the correct total. The piece you added at the end was exactly what you left off to start with. Thus when computing the amplitude of the signal (called detection), for example by multiplying it (mixing it) point by point with a constant-amplitude sine wave of the same frequency and summing the results for one cycle, the sum is independent of the starting point. That is, the result “settles” to its final value in exactly one cycle. This is in sharp contrast to any analog detection and filtering scheme. Here is why. The process of mixing two signals is mathematically identical to multiplication. For two signals of different frequency, the results (a simple trig identity) are the sum and difference of the two frequencies (heterodyne). If the two signals are of the same frequency as in the RUS numerically-implemented detection scheme described here (homodyne), the result is the sum ($2f$) and the difference, zero. The amplitude of the signal that we want is contained in either component. This is often obtained by using a low-pass analog or numerically-implemented model of an analog filter to eliminate the $2f$ component, such as a simple resistor-capacitor (RC). All such filters have some sort of continuous response to frequencies above dc. The consequence is that after a step change in amplitude of the input signal, the amplitude of the mixed signal that is reported takes some time to stabilize. For an RC filter set to $2f$ and a 16-bit digitizer, a full-scale step change in signal amplitude takes about 11 time constants to settle to one least significant bit (1 part in 65536). In contrast, summing one cycle’s worth of data from a SD signal settles in one cycle. Implementing such a scheme in a low-noise system enables one to step through frequencies to find the resonances of the specimen an order of magnitude faster than trying to emulate, or worse, actually use, an analog filter.

In an RUS system, the way SD is implemented is shown in Fig. 4, and a resonance measured with it in Fig. 5. Noting that useful specimens for RUS can be fractions of a millimeter in size with useful resonances up to 10 MHz, and that to obtain good signal-to-noise ratio a 16-or-so bit digitizer is needed to take of order 64 measurements per cycle, it is not a happy thought to try to acquire a 64 mega-sample-per-second 16 bit digitizer. So, our approach is to use a heterodyne mixer before the homodyne numerical detection just described. We generate a frequency f to drive the transmitting transducer, a frequency $f + \Delta f$ to drive an electronic analog multiplier and a frequency $m\Delta f$ to clock a digitizer. By generating a reference signal at Δf as well as the amplified transducer signal, we preserve all phase information. Using 1kHz for Δf , only a 128k samples per second (sps), two-channel digitizer is needed.

Digital process for unambiguous determination of time-of-flight (TOF) in a pulse-echo measurement

Pulse-echo (TOF) ultrasound measurements are widely used, and are thoroughly reviewed by many authors. The basic idea is to launch an acoustic pulse into a specimen and measure the time, t , it takes to reflect from the face of the specimen opposite the transducer. Then, absent many arcane corrections, $v_s = 2l/t$ where v_s is the speed of sound, l is the length of the sample, and only long division is required to process the raw data. A configuration that is in common use

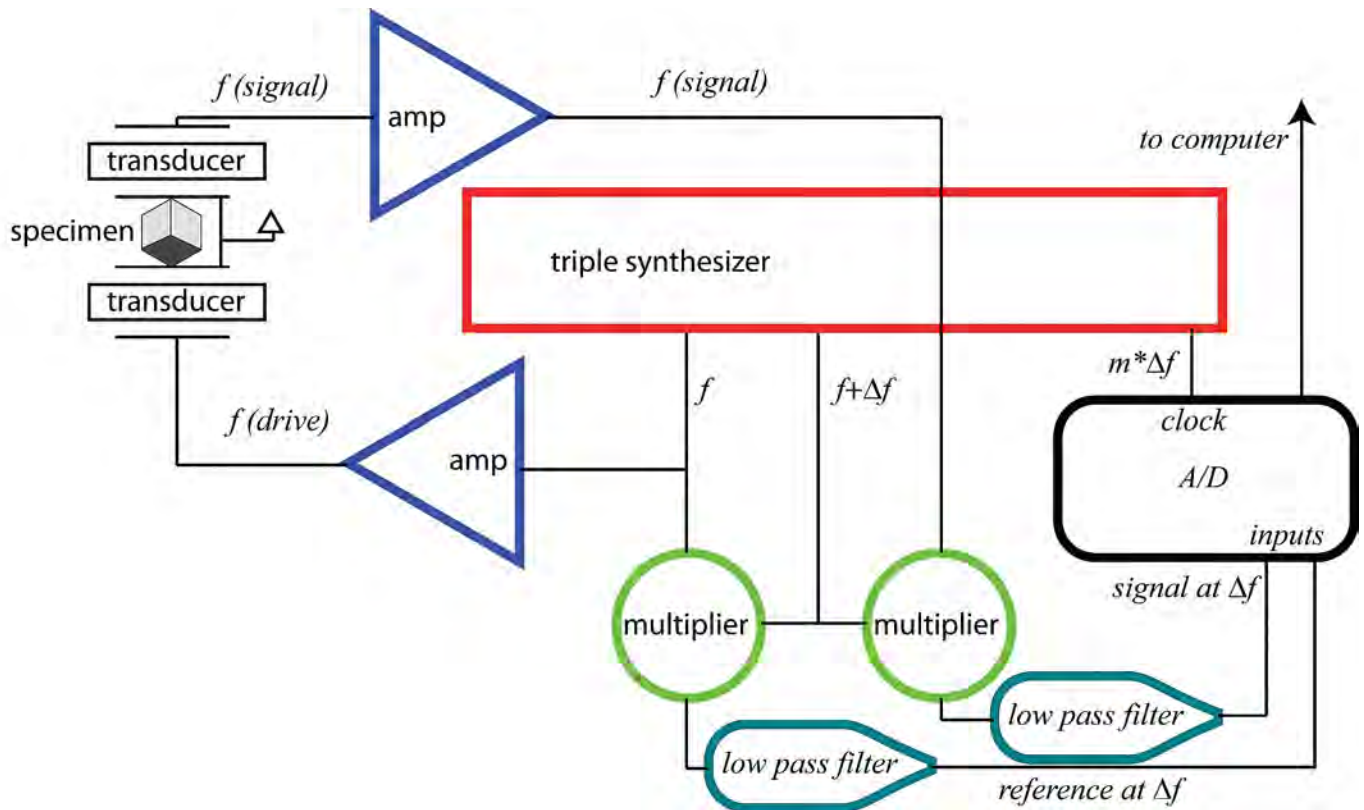


Fig. 4. Block diagram of a complete RUS system using synchronous digitization.

is to bond the specimen to a “buffer rod,” and then measure the time difference between the first echo from the buffer rod/specimen interface and the first echo from the far face of the sample, as shown in Fig. 2a. In this case, the buffer rod was a SiC anvil used in a high-pressure cell. As is clear, the sound pulse consists of a tone burst modulated by an envelope. In the simplest and least precise measurements, one measures the time difference just by looking at electronically-smoothed (detected) envelope onsets. This has poor precision because both the envelope amplitude and shape vary from pulse to pulse, and so any attempt to pick a signal level as the timing marker is doomed to produce some scatter in the result. A better approach is to retain the tone burst and “overlap” (meaning electronically multiply) it with a second

echo, and then average the result over many pulses. By registering the sinusoidal signal under the envelope of one echo, with the delayed sinusoidal signal of the second echo, much greater precision can be obtained. Registration can be achieved by adjusting the pulse repetition period to equal the time delay between echoes. The time of flight is then just the time between successive pulses. Getting this overlap correct is the issue. Without going into the many ways to electronically indicate overlap, note that as the signal strength decreases, and noise increases, it becomes increasingly difficult to determine exactly which cycle in the sinusoidal signal from the buffer rod should match with which cycle in the sample echo. If one is off by even one cycle, the answer is wrong, while all the electronics blindly report happiness. Precision is still maintained, and at low temperature and for very good signals, one can resolve variation in sound speed with temperature of 1 part in 10^8 . However, to get the absolute sound speed right, one must be certain of getting the overlap right. It turns out that a simple digital process can make the overlap unambiguous.

The trick is to use the correlation function and the frequency dependence of the overlap-determined time delay to label exactly which cycle in the sine wave is the exact right one. This process, described in detail by Pantea,⁵ begins with a very simple electronics setup. An arbitrary waveform generator is used to produce a tone burst to drive the transducer. A digital oscilloscope (A/D) captures one buffer rod echo and the one subsequent specimen echo with 8-bit/1Gs/s resolution, but with several different tone-burst frequencies. Because the A/D has a precision time base, all timing information is recorded. No further measurements are needed

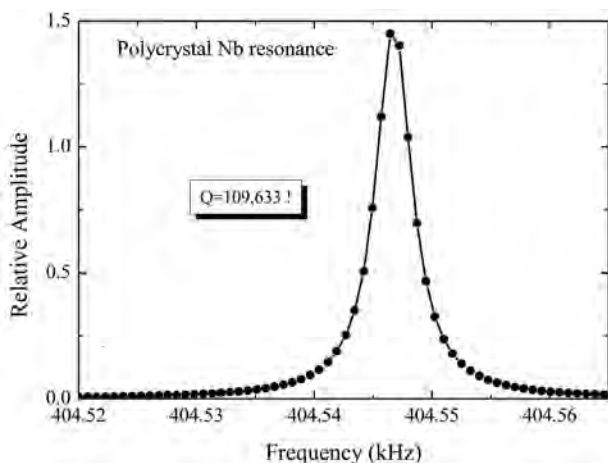


Fig. 5. A resonance acquired with the SD RUS system. The Q is 109,000.

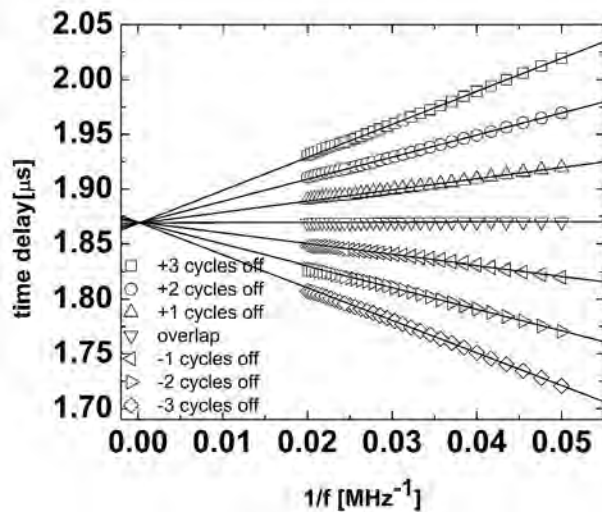


Fig. 6. The time of flight computed using the correlated signals as a function of frequency for several choices of which cycles to overlap.

while all further processing is done mathematically. The first process uses the correlation function

$$Corr(g, h, t) = \int_{-\infty}^{+\infty} g(\tau + t)h(\tau) d\tau$$

to convolute the specimen echo $h(t)$ with the buffer rod echo $g(t)$ to obtain a symmetric “pulse” that preserves the original timing information. The result is shown in Fig. 2 where the sample echo, Fig. 2b is correlated with both itself and the buffer rod echo, Fig. 2c. Next, simple fitting procedures are used to determine the time delay between the two components of Fig. 2c, but with different choices for the exact cycle of the correlated buffer rod signal (Fig. 2c left) to be used to measure the time delay to a particular cycle of the correlated S signal (Fig. 2c right). Frequency is then varied, and the computation is repeated. The results, shown in Fig. 6 show that with the correct choice for the cycles to be used to determine time of flight, the delay time is independent of frequency, and requires no user input, such as a visual guess as to what the correct overlap should be.

Thus by using a minimal electronics system without many of the complications needed for analog determination of time delays, and recording only the minimally-processed raw data digitally, it is possible to implement mathematical processes to determine unambiguously the time of flight of an acoustic pulse. The all-digital measurement of pulse-echo time of flight has the same absolute accuracy as the full inherent precision of the very best pulse-echo-overlap systems, and is simpler and cheaper than an analog-based system.

An example

Let us examine a bit of physics that begs for the use of both RUS and PE ultrasound techniques to find the answer to an interesting question. ZrW_2O_8 is a cubic material with a volume thermal expansion coefficient that is negative from liquid helium temperatures to well above room temperature.¹⁰ That is, as it warms up it contracts as if pressure were applied. This suggests an obvious measurement, that of the elastic stiffness as a function of temperature. Most materials expand on warming, accompanied by a softening of the elas-

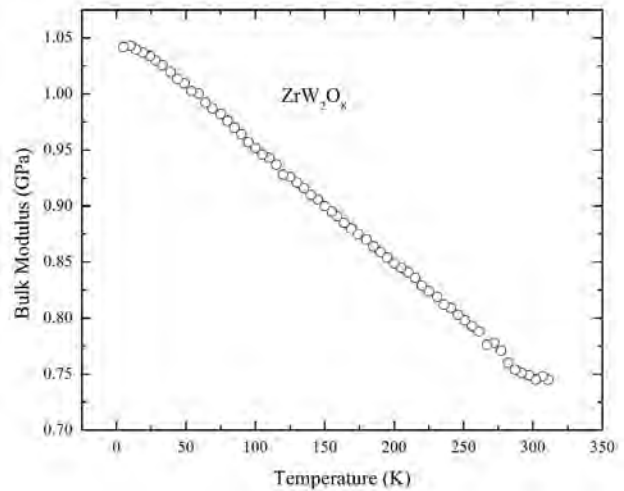


Fig. 7. Shown is the bulk modulus of ZrW_2O_8 as a function of temperature measured using the synchronous-digitization RUS system. Throughout this temperature range, the thermal expansion coefficient is negative.

tic stiffness. But if a material contracts on warming, should it not become stiffer? Using RUS we measured all the elastic moduli in one pass on a beautiful monocrystal and found that ZrW_2O_8 softens on warming¹¹ even as its volume shrinks (Fig. 7). This surprise then suggests that if one applies pressure at constant temperature, unlike most other materials, ZrW_2O_8 should get softer. But this cannot be done with RUS, and so we resorted to PE in a SiC anvil-type pressure cell,¹² bouncing sound through the anvils into the monocrystal specimen and out again. Sure enough, compressing this solid makes it softer (Fig. 8). The explanation for this is related to the famous Euler column instability problem.¹² The root of it is that even at a microscopic level, the angles and bonds among rigid substructures of the unit cell are such that heat leads to vibrations that make ZrW_2O_8 shrink like a rubber band when warmed, but under compression the same bonds begin to bend in a highly non-linear way, introducing a route to compression that is soft.^{AT}

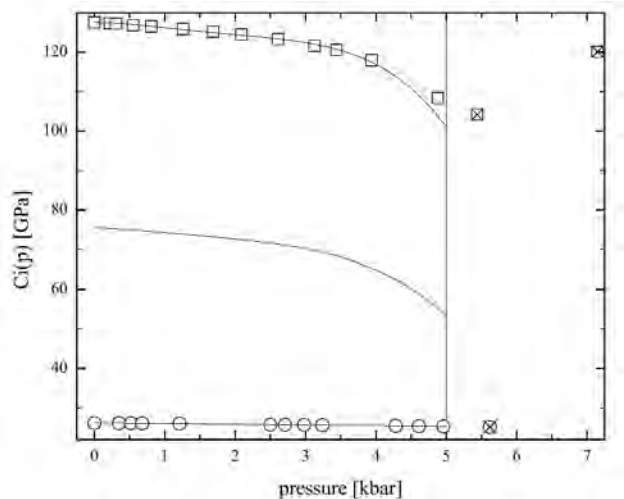


Fig. 8. The response of the longitudinal modulus and the shear modulus to pressure of ZrW_2O_8 measured in a SiC-anvil pressure cell using the digital PE system described here. Note that the material softens under compression, opposite what most materials do, but consistent with the softening that occurs on warming as the material contracts.

References

- ¹ L. D. Landau and E. M. Lifshitz, *Theory of Elasticity*, 3rd ed. (Pergamon Press, London, 1986).
- ² H. J. McSkimin, "Ultrasonic measurement techniques applicable to small solid specimens," *J. Acoust. Soc. Am.* **22**, 413–418 (1950).
- ³ A. Migliori and J. L. Sarrao, *Resonant Ultrasound Spectroscopy* (John Wiley, New York, 1997).
- ⁴ A. Migliori, J. L. Sarrao, W. M. Visscher, T. M. Bell, M. Lei, Z. Fisk, and R.G. Leisure, "Resonant ultrasound spectroscopic techniques for measurement of the elastic moduli of solids," *Physica B* **183**, 1–24 (1993).
- ⁵ C. Pantea, D. G. Rickel, A. Migliori, R. G. Leisure, J. Zhang, Y. Zhao, S. El-Khatib, and B. Li, "Digital ultrasonic pulse-echo overlap system and algorithm for unambiguous determination of pulse transit time," *Rev. Sci. Instrum.* **76**, 114902 (2005).
- ⁶ A. Migliori and J. D. Maynard, "Implementation of a modern resonant ultrasound spectroscopy system for the measurement of the elastic moduli of small solid specimens." *Rev. Sci. Instrum.* **76**, 121301 (2005).
- ⁷ E. Schreiber and O. L. Anderson, "Properties and composition of lunar materials: Earth Analogies," *Science* **168**, 1579–1580 (1970).
- ⁸ I. Ohno, "Free vibration of a rectangular parrallelepiped crystal and its application to determination of elastic constants of orthorhombic crystals" *J. Phys. Earth* **24**, 355–379 (1976).
- ⁹ H. H. Demarest, Jr., "Cube-resonance method to determine the elastic constants of solids," *J. Acoust. Soc. Am.* **49**, 768–775 (1971).
- ¹⁰ J. S. O. Evans, Z. Hu, J. D. Jorgensen, D. N. Argyriou, S. Short, and A. W. Sleight, "Raman spectroscopic study on the structure, phase transition and restoration of zirconium tungstate blocks synthesized with a CO₂ laser," *Science* **275**, 61 (1997).
- ¹¹ F. R. Drymiotis, H. Ledbetter, J. B. Betts, T. Kimura, J. C. Lashley, A. Migliori, A. P. Ramirez, G. R. Kowach, and J. Van Duijn "Monocrystal elastic constants of the negative-thermal-expansion compound zirconium tungstate (ZrW₂O₈)," *Phys. Rev. Lett.* **93**, 025502-1 (2004).
- ¹² C. Pantea, A. Migliori, P. B. Littlewood, Y. Zhao, H. Ledbetter, J. C. Lashley, T. Kimura, J. Van Duijn, and G. R. Kowach, "Pressure-induced elastic softening of monocrystalline zirconium tungstate at 300 K," *Phys. Rev. B* **73**, 214118 (2006).



Albert Migliori received a B.S. in physics in 1968 from Carnegie Mellon University and M.S. and Ph.D. degrees in physics from the University of Illinois in 1970 and 1973. He is associate director of the Seaborg Institute for Actinide Science at Los Alamos National Laboratory. Dr. Migliori is co-discoverer of acoustic heat engines. He is

a leading expert in the use of resonant ultrasound spectroscopy as a solid-state physics tool for which he won R&D Magazine's R&D 100 Awards in 1991 and 1994. He has also won a Federal Laboratory Consortium Award for Excellence in Technology Transfer in 1993, and a Los Alamos National Laboratory Distinguished Performance Award in 1994. He is a fellow of the Los Alamos National Laboratory, the American Physical Society, and the Acoustical Society of America. He holds 25 patents, is the author of over 200 publications, six book chapters, and one book. Recent interests include elasticity of Plutonium, superconductivity in pulsed magnetic fields, and state-of-the-art research and development of new measurement techniques.